Imaging Common Shot Gathers

Bert Jacobs

Abstract

Common shot gather imaging is done because the shot-geophone coordinate system is probably the best system in which to work when trying to estimate a laterally varying velocity function. Shot-geophone coordinates also have advantages when the shot axis is aliased. Within a shot gather, the data is a function of time and offset. Migration is easier after NMO correction and a time-to-depth conversion, since all that is involved is the application of small shifts to the dipping events in the moveout corrected gather. These shifts are in both the vertical and lateral directions. A natural coordinate system for describing an NMO and time-to-depth corrected gather is the radial/NMO coordinate system.

Introduction

Seismic data is collected in shot-geophone coordinates and is almost always processed in the offset-midpoint coordinate system. Offset-midpoint processing works best when sampling along the shot axis is not too sparse, when lateral velocity variations are absent, and when each of the interfaces in the subsurface has a fairly uniform dip. Alternatively, if the data truncation problem can be solved and if fairly good velocity estimates are obtainable, then downward continuing common shot gathers should be a reasonable alternative to stacking moveout-corrected common midpoint gathers. Downward continuation of common shot gathers is a process independent of both reflector geometry and shot coordinate sampling. It is also a process that can incorporate most acoustic velocity structures.

Consider first the effect of shot aliasing on the migration of stacked seismic sections. The midpoint sampling rate is equal to half the group interval and is actually independent of the distance between shots, so the problem must be subtle. Assuming that the group interval is small enough to prevent aliasing of data in the common shot gathers, the problem gets

more severe as shot space increases. Starting with the situation in which the shot spacing is equal to the group interval, the common midpoint gathers in this case can be partitioned into two classes since it turns out that there are two near offset distances among the set of common midpoint gathers. As the shot spacing is increased further and further, the multiplicity and range of near offset distances increases as does the common midpoint coverage. It is to be expected that the quality and coherence of the stacked sections of such a data set will decrease as the coverage decreases and the common midpoint gathers become more and more dissimilar. In the limiting case in which the shots are infinitely far apart, the common midpoint gather and stacked section are useless abstractions. Even in this case, we know that we can (with a ray tracing program and some geological insight) get some idea of the structure of the earth immediately below each of the isolated common shot gathers.

Consider next the effect of a fairly rapid lateral change in acoustic velocity above a simple geology on a common midpoint gather. For instance, consider a marine survey over a layered earth in an area where the acoustic velocity gradients are small. To get the simplest sort of model, assume that only one reflector other than the sea floor is present and that the trace length is such that the first sea floor multiple is not recorded. All the common midpoint gathers of the survey will be the same. Each such gather contains a direct wave, a hyperbolic event due to the sea floor reflection, and a hyperbolic event due to the primary reflection from the sub-sea floor horizon. If the model is changed so that the sea floor has significant topography and so that the acoustic velocity of the floor sediments are significantly different from the velocity of sound in sea water, then the reflection seismograms become more complicated. In particular, the common midpoint gathers will not be identical, and the two seismic events on each midpoint gather will not always be hyperbolic.

Uniform dip has negligible effect on the quality of common midpoint stacks. Consider a suite of common midpoint gathers recorded over a uniformly dipping reflector. Each such gather has a single hyperbola on it, and each of these hyperbolae can be characterized by its zero offset travel time and its asymptote. The zero offset times progressively, and predictively, decrease as the survey proceeds up-dip. At the same time, the slopes of the asymptotes remain constant and equal to the the cosine of the dip divided by the rms velocity to the reflector horizon. If the dip of the reflector is very non-uniform, then the reflection event on at least some of the common midpoint gathers will be non-hyperbolic. Again, some degradation in the quality of the common midpoint stacks is expected.

A Spectrum of Common Shot Gather Imaging Techniques

There are many ways in which to get approximate images of the subsurface while working in the shot-geophone coordinate system. For instance, either the geophones alone can be downward continued or both the shots and geophones can be extrapolated into the subsurface. Once that decision has been made, the choice of coordinate system in which to migrate is still arbitrary. A given coordinate system may still allow the processor to choose between phase shift, FK, or finite difference implementations of the one-way wave equation.

A processing technique which is independent of both acoustic velocity and reflector geometry has to involve some sort of migration before stack. If the acoustic velocity is allowed to vary significantly over small regions of space, then that migration before stack will probably have to be done in shot-geophone coordinates. At this point, one has the choice of downward continuing common shot gathers, common geophone gathers, or both. Downward continuing both the shots and the geophones simultaneously destroys the redundancy of the data set. Whereas a seismic line contains views of the earth from many angles, the output of a shot-geophone migration migration algorithm collapses these to a single estimate of earth structure. On the other hand, common shot gather migration generates many different estimates of earth structure which can be compared with one another. Any differences between these estimates can (hypothetically) be translated into perturbations of the model parameters, the values of the acoustic velocity function.

The choice of how to migrate a suite of common shot gathers is an economic one, determined by what is known of the geological setting (i.e. the presence of large dips, significant vertical velocity variations, and/or lateral velocity variations), what is desired of the migrated output (for example, qualitative geology, the estimation of thickness of a producing layer, and the spatial positioning of a well target near a salt dome require increasingly sophisticated algorithms), by the dollar value attached to the output when oil is expected, and by estimates of the processing cost. All the common shot gathers need not be processed with the same algorithm. In fact, not even all the z-steps within any given common shot gather need to be taken in the same way.

For economic reasons (in the absence of an algorithm which is both cheap and general) a processing sequence for seismic lines must rely on an inexpensive routine to do most of the work. This cheap program should be expected to behave well only in the simplest geological settings. In our case, this setting consists of flat reflectors embedded in a medium whose velocity is a function of depth only. If shot gathers whose migration requires a laterally varying velocity function are found, then one can easily back up and apply a more expensive and specialized algorithm to improve the image. We are lucky, because there is a small spectrum of cheap algorithms to choose from.

The cheapest way to get an approximate image of the subsurface from a common shot gather is to perform a time-to-depth conversion on a normal moveout corrected gather. The offset axis has to be reinterpreted since the reflections occur at points whose lateral positions are an average of those of the shots and geophones. The reflection points sample space at twice the density the geophones do. Their near offset relative to the shot is half that of the geophones. If the group interval and near trace distance on input are Δg and g_0, respectively, then the output should be a approximate image of the subsurface with spatial sampling interval $\Delta g / 2$ and near offset $g_0 / 2$.

One step up in cost from NMO is a pre-stack migration of an NMO corrected common shot gather. If there are segments with small dips present, then migration should shift these segments upwards and a little to the side. The advantage gained by migrating consists of improvements in the estimates of the spatial positions of the reflectors in the subsurface. The correction involved in the migration of NMO corrected common shot gathers is probably of much greater importance than the pre-stack migration of common midpoint gathers, since uniformly dipping reflectors can be stacked in CMP gathers without any pre-stack migration correction.

There are at least two geological settings in which an NMO-based algorithm, such as the algorithms sketched above, will fail. One setting involves bad velocity functions and the other is due to steep dips. If the acoustic velocity function changes too quickly, then there will not be a uniquely defined NMO correction at the far offsets of either common shot gathers or common midpoint gathers. If steep dips are present below a section of the survey then normal moveout will not even come come close to correcting for the observed stepouts. A common shot gather which cannot be NMO corrected can still be imaged. Perhaps the cheapest process that will do this is phase shift migration. Unfortunately, this algorithm requires that its input data be unaliased. This is not a problem along the time axis, but is a major problem along geophone axis. Two ways around the aliasing problem are interpolation and the choice of a slant coordinate system for migration in which stepouts are smaller.

Normal Moveout and Time-to-Depth Conversion

The NMO method of imaging was performed on 86 successive gathers from a marine seismic line from the Gulf of Alaska provided by the USGS. The parameters of the recording geometry are listed in table 1. A near trace section and a plot of the first five seconds from the first eight common shot gathers appear in figures 1 and 2, respectively. Both have been plotted with a linear gain and clipped at the 99-th percentile.

Number of groups	48
Group interval	50 m
Number of shots	86
Pop interval	50 m
Near offset	238 m
Trace size	2500
Sampling rate	4 msec
V_0	1480 m/s
Sampling rate for r	0.011261 msec/m
Sampling rate for d	18.5 m
Migration step size	185 m
Output number of groups	48
Output group interval	50 m
Output near offset	-643.5 m

TABLE 1. Input and migration parameters

The near offset section should be examined carefully, because an understanding of its geometry will come in handy when it is time to interpret the common shot gathers. The first fact to note is that no effort was made to remove either the bubble waveform or multiple reflections from the data. All attempts at bubble deconvolution decreased the lateral coherence drastically. On the other hand, multiples were left in the data to study their behavior under common shot imaging processes. Since the water is roughly 1.85 kilometers deep, the first few primary reflections and their sea-floor multiples are well separated from one another. If the events on the section are identified by their time of occurrence on trace number 86, the left-most trace, then a sea-floor primary can be identified at 2.2 seconds. The sea-floor reflection has several diffraction hyperbolas superimposed on it reflecting a rough topography. The sea-floor reflection occurs at an earlier times as the shot point index increases, corresponding to a sea-floor dip of approximately five degrees. Additional primary reflections occur at 2.6 and 3.4 seconds. The primaries have lateral amplitude variations which might be due to the focusing and defocusing of the irregular sea-floor. The primaries also have an apparent dip which seems to be largely due the lateral variation in the size of the water column. Sea-floor multiples occur at 4.4 and 4.8 seconds on trace 86.

The water bottom reflection at 2.6 seconds and primary reflections at 3.0 and 3.5 seconds are easily identifiable on the common shot gathers. The multiple is absent on the gathers of figure 1, because it is expected to occur at times later than 5.2 seconds in this part of the line. The multiple can, however, be observed to creep into the bottom of gathers from later in the line when these are displayed. Such displays are easily made in movie form for display on a storage screen.

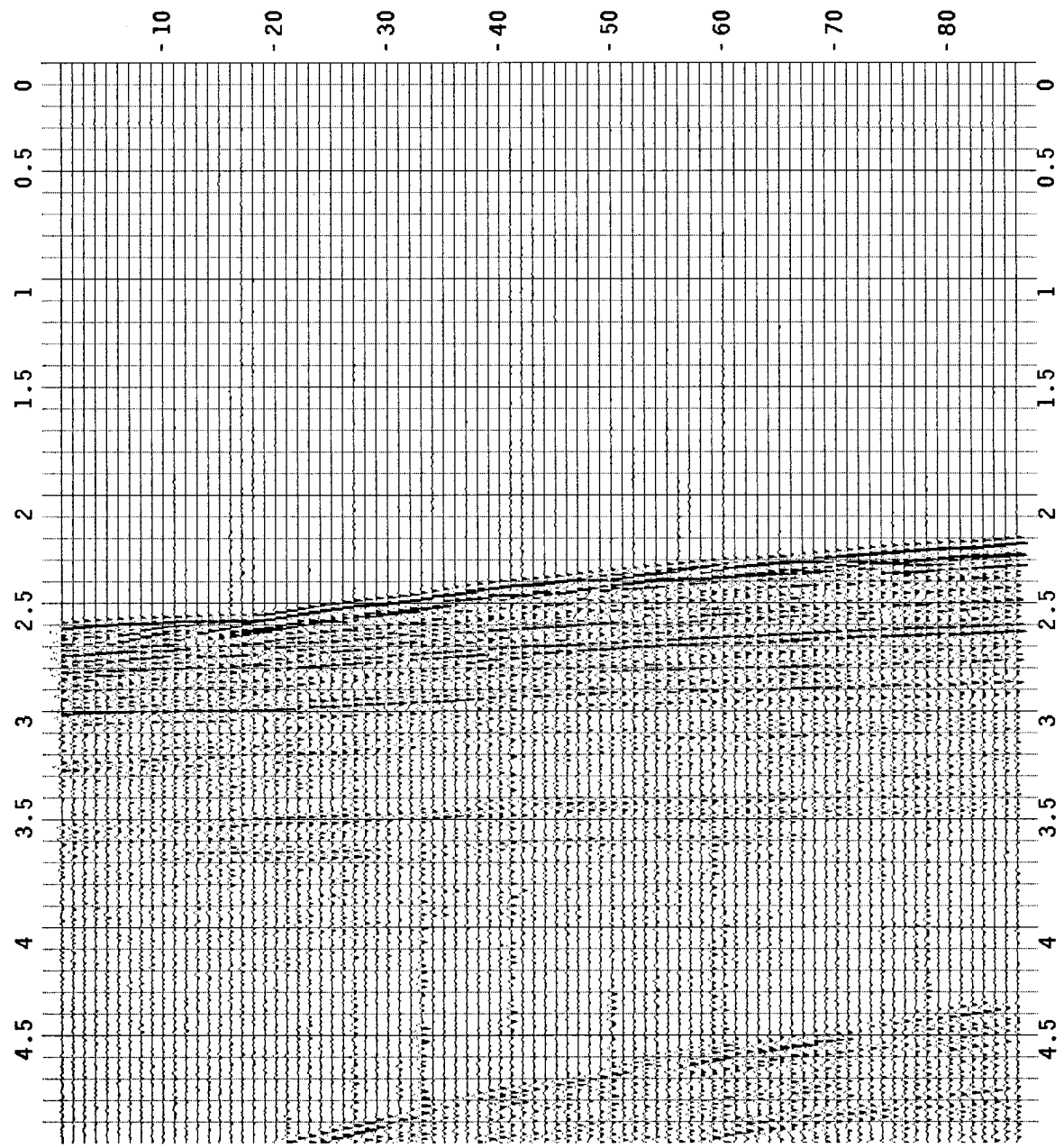

FIG. 1. A near offset section from a line recorded in the Gulf of Alaska by the USGS. The vertical axis is labeled with time in seconds, while the horizontal axis is labeled with shot number. Each shot is separated by a pop interval of 50 meters.

Fortunately, the seismic line was accompanied by the results of rms velocity measurements from several of the midpoints. From these, a reasonable rms velocity function was formed for the section of the line from which figure 1 was constructed. It is displayed in figure 3, with time on the horizontal coordinate. By performing normal moveout and a time-to-

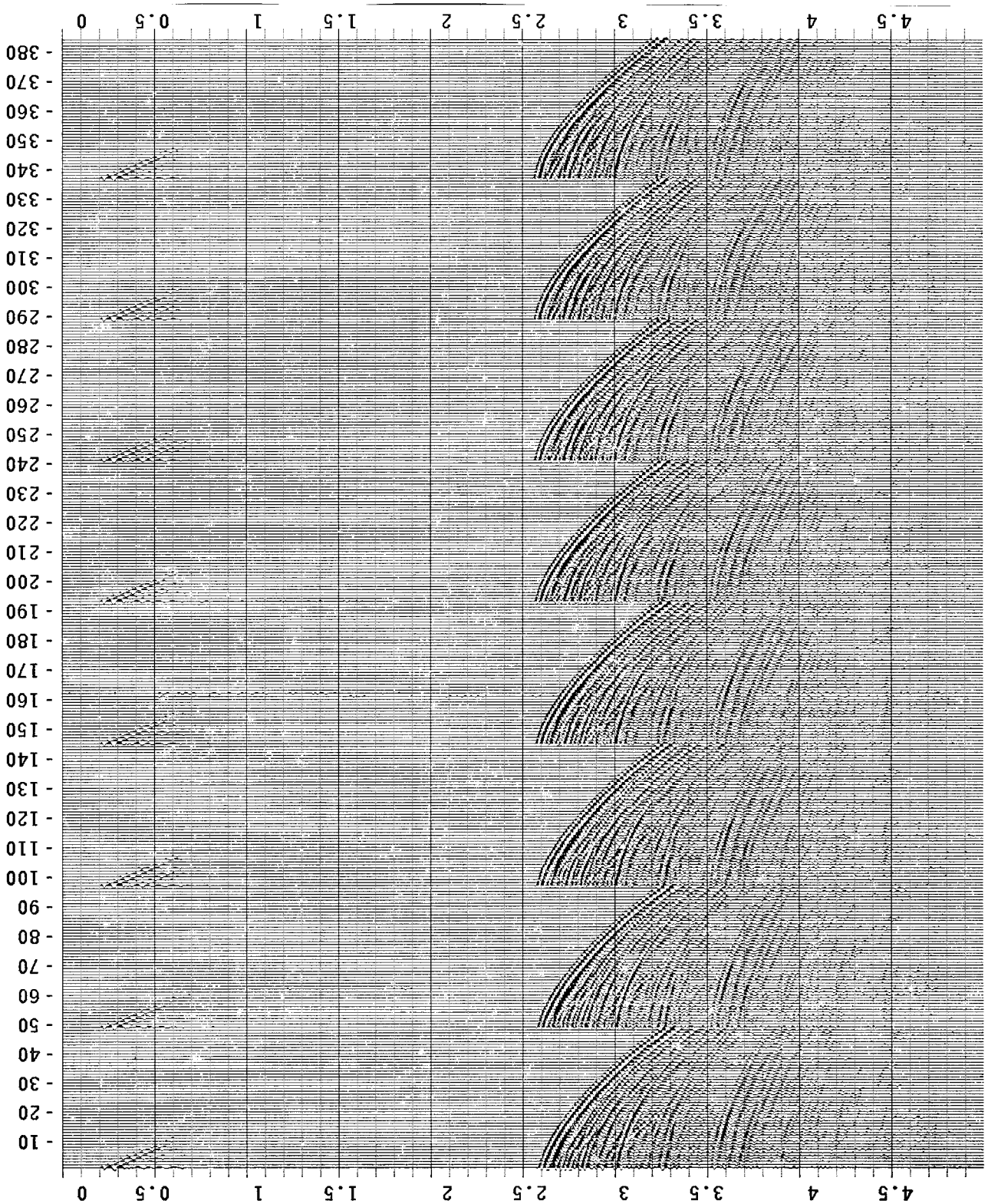

FIG. 2. The first eight gathers of the USGS Gulf of Alaska line. The first traces from each of these gathers are also the left-most traces displayed in figure 1. The scale on the vertical axis is in seconds.

depth conversion, an estimate of the positions of the reflectors beneath the shot gathers can be made. The result for the first eight gathers is plotted in figure 4. The output has been effectively subsampled deleting every other trace to make it look more like figure 14, a plot of the same common shot gathers after wave equation migration.

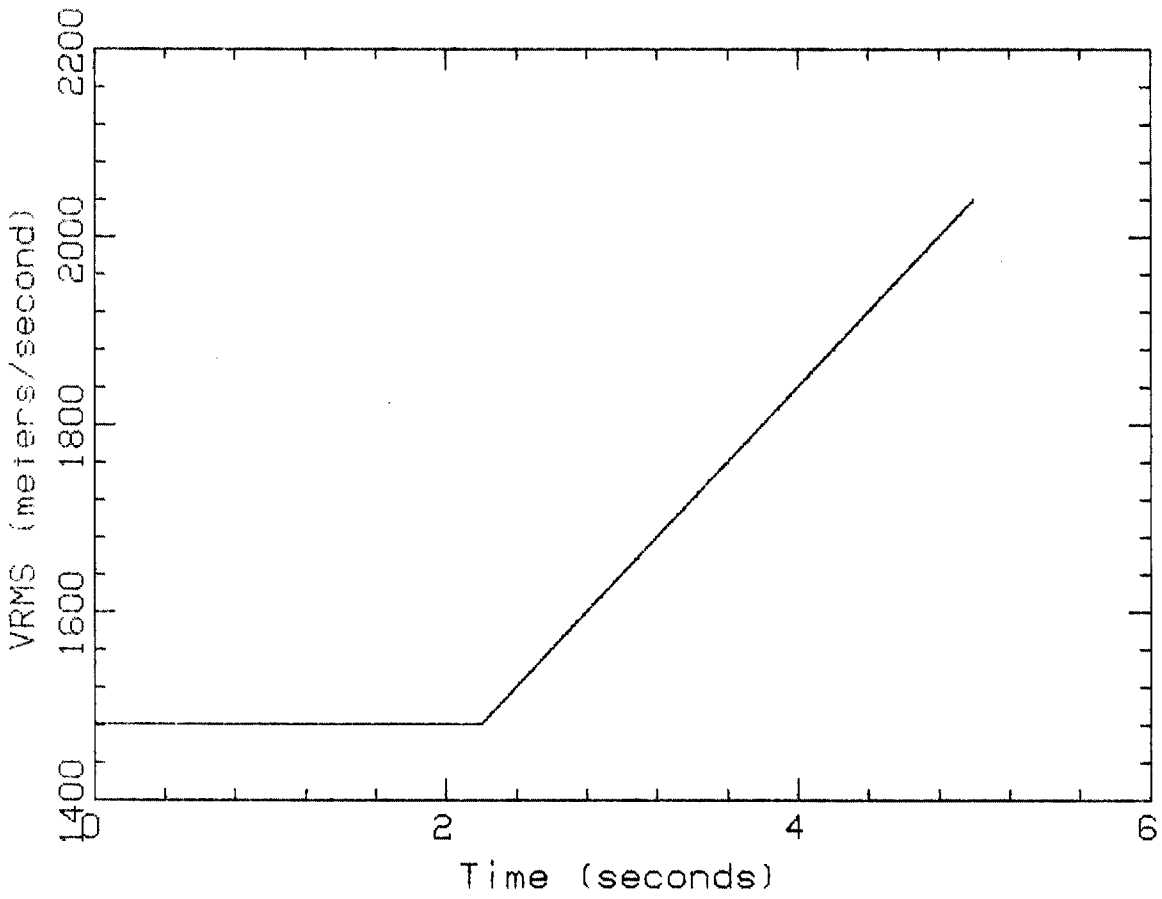

FIG. 3. The RMS velocity function used to NMO correct the data plotted in figure 2.

(actually figure 4 was generated by passing the data through every step of the migration procedure used to generate figure 14 except those steps involving data extrapolations at near and far offsets and the step involving an application of the 15-degree wave equation operator). The padding in figure 4 was put there for the same reason, to make the job of comparing migrated and unmigrated NMO corrected common shot gathers easier.

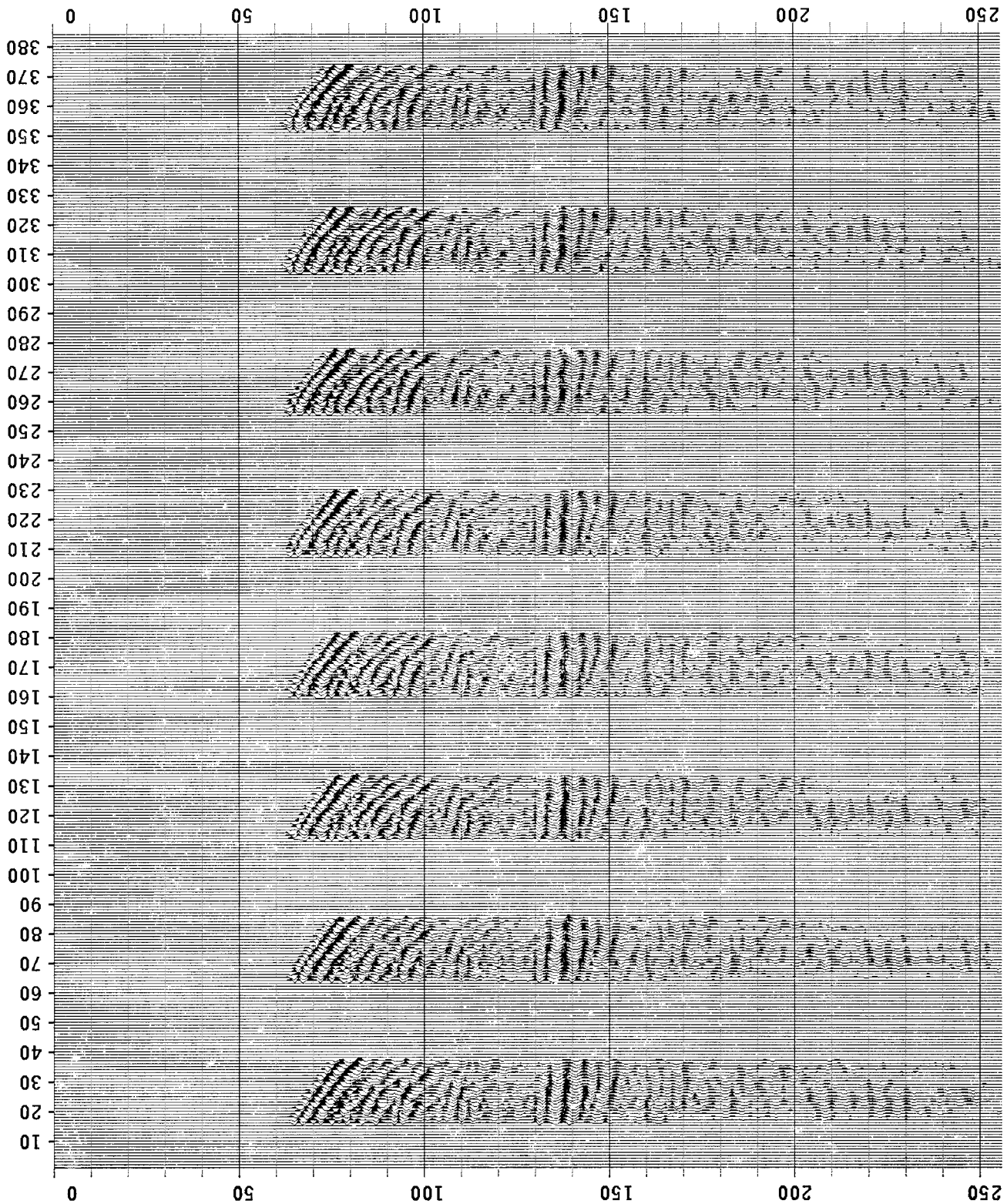

FIG. 4. The first eight gathers of the USGS Gulf of Alaska line. The gathers have been NMO and time to depth corrected, and then windowed so that the sediments could be more carefully observed. The first depth plotted is the 49th sample at 888 meters.

The Radial/NMO Coordinate System for Imaging Gathers

The data that is most likely to be aliased on a common shot gather recorded in an area with only small deviations from layer cake geology is that lying at large offsets. Normal moveout alleviates the problem for primary reflections from planar interfaces with near-zero dip. A cursory comparison of figures 2 and 4, for instance, shows that the range of stepouts has been markedly reduced by applying a normal moveout correction. If a normal moveout coordinate system is used for migrating seismic data recorded over a favorable geology, then the job of migration is easy and amounts to a time-to-depth conversion plus a small amount of lateral and vertical shifting. The job is so easy that a low order (15-degree) differential equation with a large step size can be used. The use of a 15-degree equation with a large step size makes for a pre-stack migration at cut-rate cost.

Another way to decrease the effort involved in pre-stack migration is to use a radial coordinate system. The ray parameter of a ray propagating in a layer cake-like earth is an invariant function of the depth. Thus, if radial coordinates are used for migrating events due to reflectors with near-zero dips, then a migration will involve some vertical shifts and still smaller "lateral" shifts of energy from one ray coordinate value to neighboring ray parameters.

The simultaneous use of a radial and NMO coordinates for the migration of data recorded over a regions with small dips should involve a minimum of effort. Moreover, the use of radial coordinates eases the boundary condition problem at the far offsets, since a boundary condition that forces the wavefield to equal zero at the ray parameter corresponding to horizontal propagation is a natural one. The other side boundary still presents a problem. In this study, a zero-slope boundary condition was enforced at the small-r side of the data while it was downward continued.

The easiest way in which to visualize the radial/NMO coordinate system is to check figure 5. The new coordinate system requires the specification of a constant velocity parameter v_0. In terms of v_0 and $h = g - s$, the transformation from the offset-time-depth coordinate system to radial/NMO coordinates is a set of three equations:

$$\begin{aligned} r &= \frac{h}{v_0^2\, t} \\ d &= \frac{1}{2}\left[z + \left(v_0^2 t^2 - h^2\right)^{1/2}\right] \\ z' &= z \end{aligned} \tag{1}$$

The inverse transformation, form radial/NMO coordinates to recording coordinates, is easier to visualize. It is also more important, since the computer implementation of the algorithm for

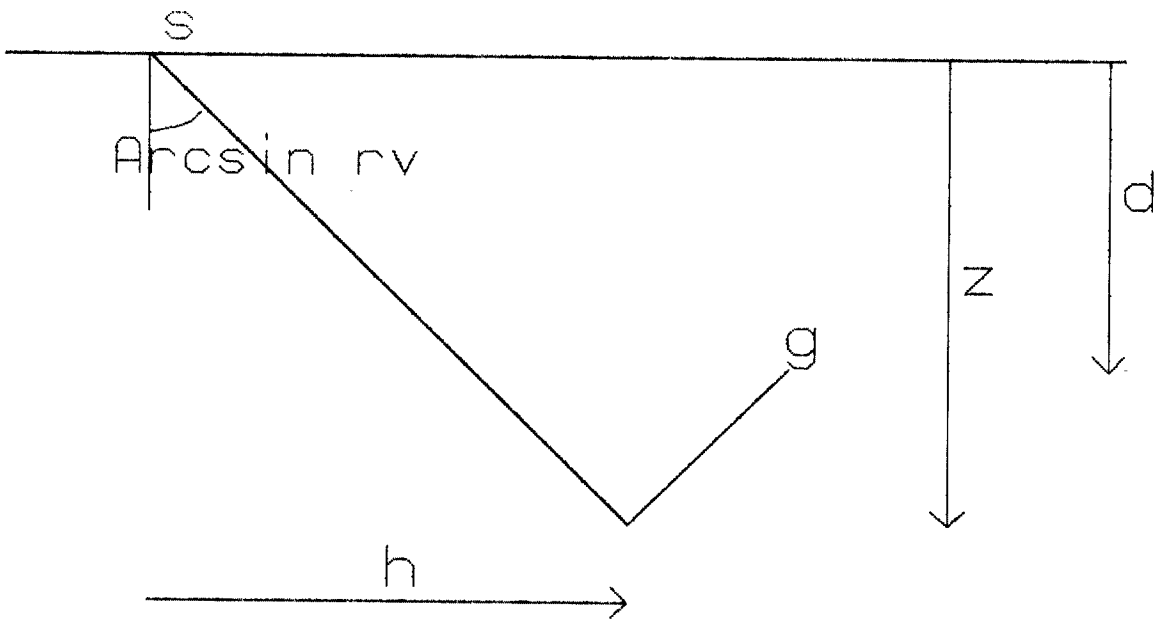

FIG. 5. Recording coordinates are the distance from shot to phone h, the depth of the phones z, and the travel time from shot to reflector to geophone t. Radial/NMO coordinates are the sine of the angle of propagation r, the depth of the phones z, and reflector depth d.

migrating NMO corrected common shot gathers in radial/NMO coordinates uses the inverse transformation to map the data into radial/NMO space. Again there are three equations to contend with:

$$\begin{aligned} h &= \frac{(2d - z')\, r\, v_0}{\left(1 - r^2 v_0^2\right)^{1/2}} \\ t &= \frac{2d - z'}{v_0\left(1 - r^2 v_0^2\right)^{1/2}} \\ z &= z' \end{aligned} \tag{2}$$

When $z' = z = 0$, implementation involves finding, for each pair r_0,d_0 in the output space, the value of the input field at the corresponding pair h_0,t_0, given by the inverse transformation of equation 2. In general h_0,t_0 will not be a grid point of the input, so some kind of interpolation will be necessary. All the examples of this section used a four point linear interpolation scheme to interpolate along a line in h,t space. This line is chosen so

that is the tangent to the zero-dip reflector travel time curve through h_0,t_0. The slope of such a line is easily found to be equal to $h/(v_0^2 t)$. Not coincidentally, this slope is identical to r.

The Radial/NMO 15-Degree Wave-Equation

A common shot gather in any coordinate system can be treated as a boundary condition for a one-way wave equation. If that one-way wave equation is the 15-degree equation, then it can be written in radial/NMO coordinates by using the chain rule. From equations 2, the substitutions

$$\begin{aligned}
\frac{\partial}{\partial g} &= \frac{1}{v_0}\frac{\left(1 - r^2 v_0^2\right)^{1/2}}{(2\,d - z')}\frac{\partial}{\partial r} - \frac{1}{2}\frac{r v_0}{\left(1 - r^2 v_0^2\right)^{1/2}}\frac{\partial}{\partial d} \\
\frac{\partial}{\partial t} &= -\frac{r v_0\left(1 - r^2 v_0^2\right)^{1/2}}{2\,d - z'}\frac{\partial}{\partial r} + \frac{v_0}{2}\frac{1}{\left(1 - r^2 v_0^2\right)^{1/2}}\frac{\partial}{\partial d} \qquad (3) \\
\frac{\partial}{\partial z} &= \frac{1}{2}\frac{\partial}{\partial d} + \frac{\partial}{\partial z'}
\end{aligned}$$

must be made to express the one-way wave equation for upgoing waves in radial/NMO coordinates. For a constant acoustic velocity v_0 the one-way wave equation for an upwards propagating wavefield P in a single shot experiment takes the form

$$\frac{\partial P}{\partial z} = \left(\frac{1}{v_0^2}\frac{\partial^2}{\partial t^2} - \frac{\partial^2}{\partial g^2}\right)^{1/2} P \qquad (4)$$

The direction of propagation is controlled by the manner in which the square root is defined. Following time-honored SEP tradition, the square root of an operator is defined by its continued fraction. Thus, if A and B are operators, B is positive-definite, and A is positive (negative) semi-definite, then $(A + B)^{1/2}$ is an operator which is positive (negative) semi-definite. When A is strictly imaginary, the square root is taken to be non-negative imaginary. Thus, the square root in equation 4 is causal in the t-direction when the time derivative is a causal derivative, and is anti-causal when the time derivative employed is an anti-causal derivative.

Substituting equations 3 into equation 4 yields a partial differential equation for propagating upgoing waves in radial/NMO coordinates. If first derivatives of the wavefield are ignored, and the primes on z' are dropped, then differential equation 4 looks like

$$\left(\frac{\partial}{\partial z}+\frac{1}{2}\frac{\partial}{\partial d}\right)P \;=\; \left[\frac{1}{4}\frac{\partial^2}{\partial d^2}-\frac{\left(1-r^2v_0^2\right)^2}{v_0^2(2d-z)^2}\frac{\partial^2}{\partial r^2}\right]^{1/2}P$$

in the new coordinate system. Dropping the first derivatives of the wavefield leaves the phase behavior of the 15-degree approximant intact, but does alter the amplitude behavior. Since we are much more interested in timing shifts for velocity analysis and for good stacks, dropping these first derivatives leaves the 15-degree equation unaltered for all practical purposes. The square root can, as usual, be expanded as a continued fraction. If the continued fraction is truncated at any of its partial and if the partial denominators of the truncated fraction are cleared, the result is a partial differential equation which behaves much like a wave equation. The result of truncating at the first partial denominator is

$$\frac{\partial^2}{\partial d\,\partial z}P \;=\; -\frac{\left(1-r^2v_0^2\right)^2}{v_0^2(2d-z)^2}\frac{\partial^2}{\partial r^2}P$$

which looks like the 15-degree equation geophysicists have become used to. The differences are that the coordinate system has been changed and the coefficient in front of the second derivative with respect to the lateral "spatial" coordinate is no longer a constant.

The direction of propagation of equation 4 is defined, but its causality is not. The equation can be used to push an upgoing wavefield either downwards or upwards. Migration pushes the upgoing wavefield downwards, and does this by specifying the causality of the z and d derivatives that it uses. Anti-causal derivatives are used, denoted in the notation of previous SEP reports by $(-D_z)^H$ and $(-D_d)^H$, respectively. Migration also makes use of both causal and anti-causal lateral derivatives, D_r and $(-D_r)^H$, respectively. With these conventions, the 15-degree wave equation for migrating upgoing waves is

$$(-D_d)^H(-D_z)^H\,P \;=\; \frac{1-r^2v_0^2}{v_0(2d-z)}\,(-D_r)^H D_r\,\frac{1-r^2v_0^2}{v_0(2d-z)}P \qquad (5)$$

where the right hand side has been altered to make the migration differential equation stable. Since the right hand side of equation 5 has functions which are d-dependent, a Fourier transform over d does not lead to a simple frequency domain formulation of the wave equation. Hence, equation 5 was discretized and implemented in the d (time-like)-domain.

The Imaging Condition in Radial/NMO Coordinates

The discrete version of equation 5 is applied recursively in the anti-causal d and z directions, much as the old 15- or 45-degree time domain operators in x,z,t- space worked in the anti-causal t and z directions. Migration, therefore, sweeps energy into regions of earlier d and shallower z. From figure 5, it can be seen that an image is obtained where the geophone depth z is equal to the reflector depth d and at a time equal to the travel time from the shot to the image point. Hence the imaging condition, expressed in a mix of coordinate systems, is

$$d = z \qquad t = \frac{1}{v_0}\left(z^2+h^2\right)^{1/2}$$

where $h = g - s$, as before. These two equations can be written in terms of radial/NMO coordinates only, if equations 1 are used. The image which is destined to appear at lateral position h and depth z appears at positions in r,d,z-space given by

$$d = z \qquad r = \frac{h}{v_0\left(z^2 + h^2\right)^{1/2}} \tag{6}$$

Thus, the image is a linear subset of the plane $d = z$, parallel to the r axis. This subset can be mapped into recording coordinates h,z through a simple resampling and mapping procedure.

The range over which h is allowed to sweep is still arbitrary. An option that works well is to let h range over a segment about as long as the input data. The near offset distance should be at most equal to half the near offset distance before migration, less some length for padding. The output should probably include some traces with negative offsets.

The Transformation and Migration of Common Shot Gathers

The pre- and post-processing for common shot gather migration is complicated and involves many steps. Plots of some of the steps are invaluable in judging the propriety of the many approximations used by a radial/NMO migration algorithm.

The new coordinate system is defined in terms of a constant transformation velocity, so the first problem that arises is that of coping with vertically varying acoustic velocity. The solution attempted here is to convert the input data so that it looks like a common shot gather recorded over a constant velocity earth. This can be achieved by applying an NMO correction with a time varying rms velocity function, converting from time to depth, and then applying an inverse NMO correction with a constant transformation velocity v_0. Figures 6

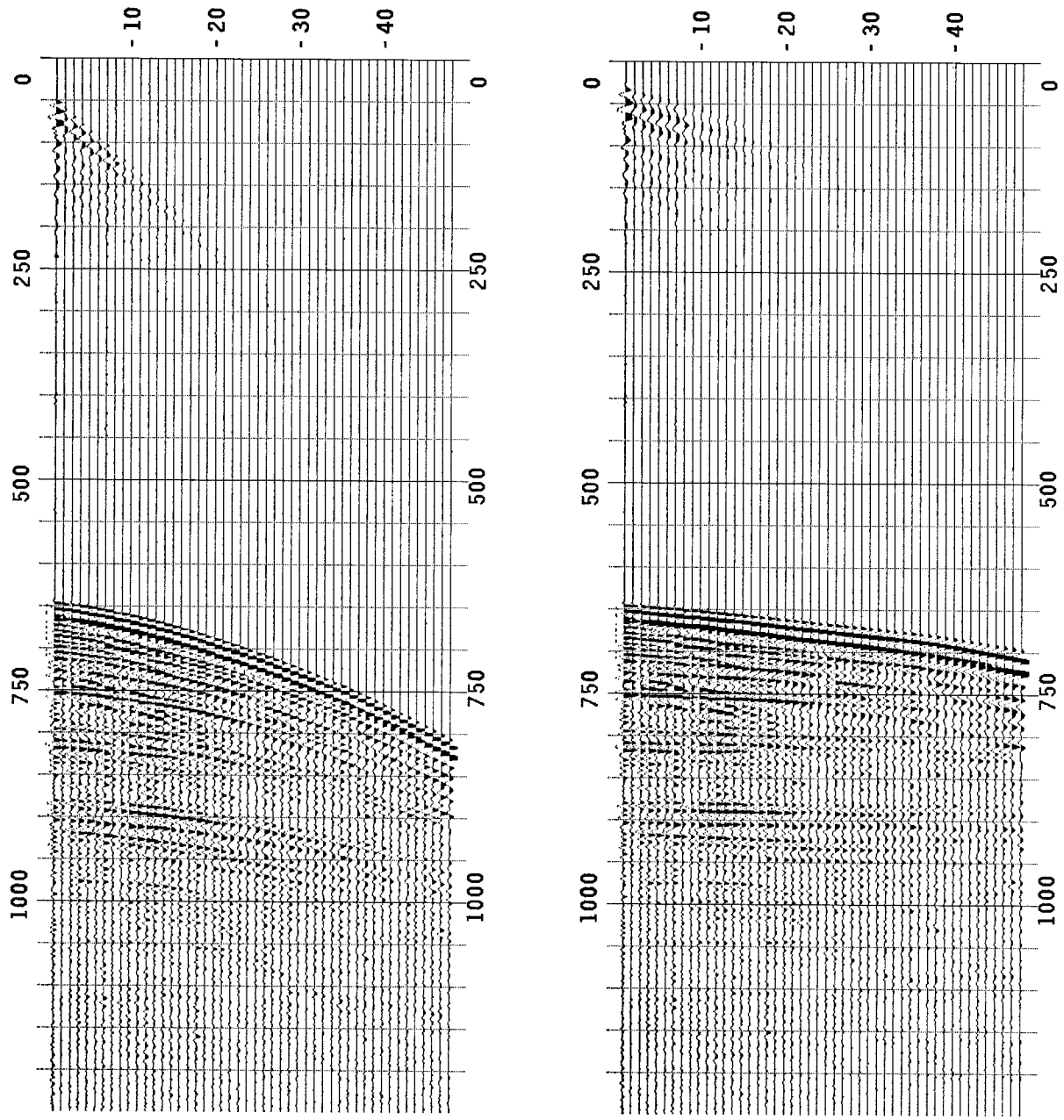

FIG. 6-7. Left: A plot of the input. Right: The input has been NMO corrected with the figure 3's rms velocity.

through 9 illustrate this step, as applied to the left-most gather of figure 2.

After conversion into a constant velocity gather, some pre-processing is still needed to lessen the effect of near and far offset data truncations. The data is therefore padded and the padding filled with an extension of the original data. In figure 10 the 48 traces of the input have been padded with six traces of zeros on the left and six traces of zeros on the

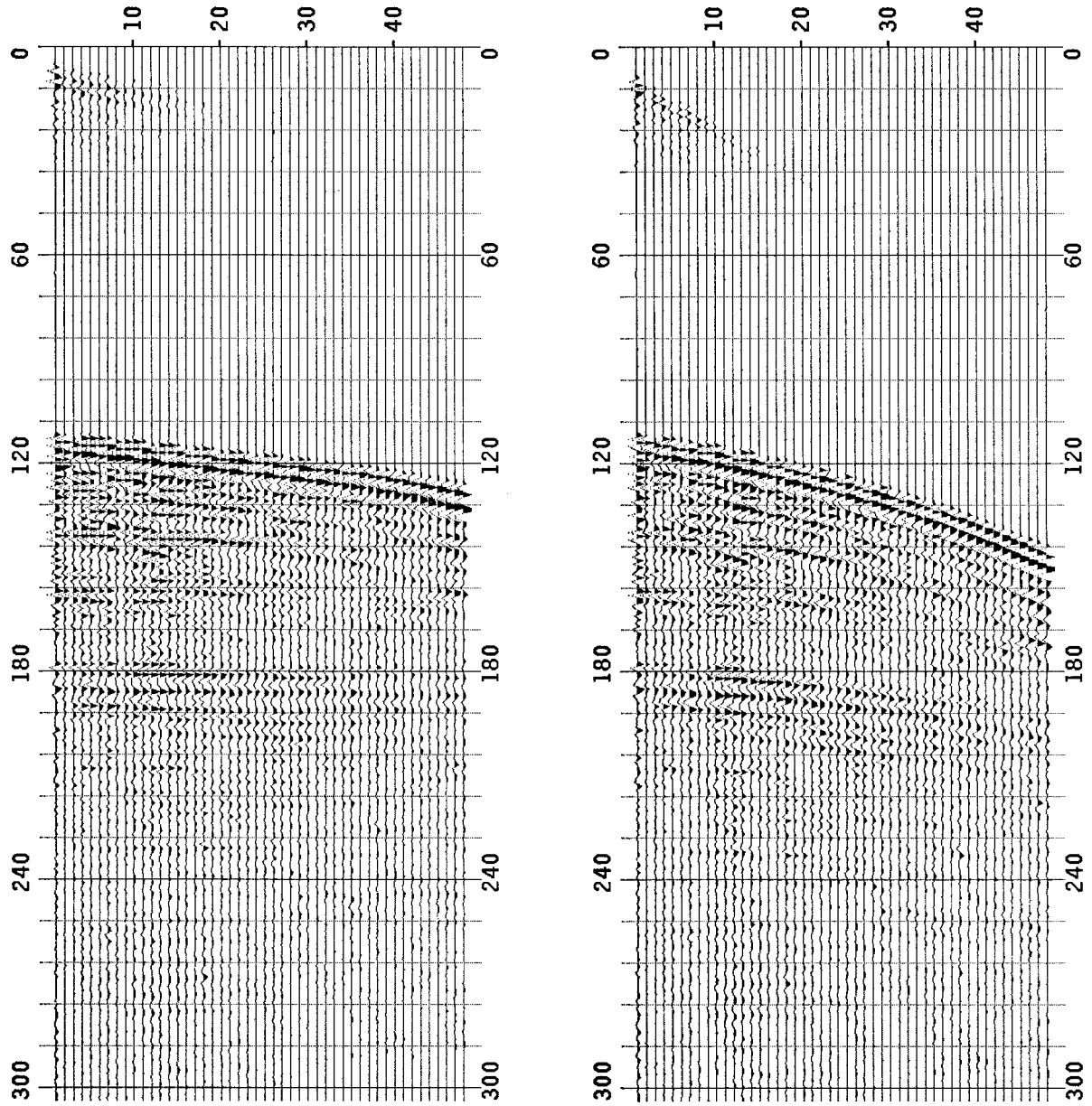

FIG. 8-9. Left: the result of applying a time to depth conversion routine to figure 7. Right: the result of a subsequent application of a constant velocity inverse NMO correction. A transformation velocity of 1480 m/s was used.

right. The bottom was padded with a mere four samples. The padding was filled in by (1) applying a spherical divergence conversion to make the data more stationary, (2) applying a normal moveout correction to reduce the range of stepouts and change most events so that they are linear and horizontal, (3) transposing the NMO corrected data, (4) convolving the

transpose with a time-domain recursive dip filter set to reject high dips, (5) transposing the filtrate, (6) restoring the normal moveout, (7) restoring spherical divergence, and (8) restoring the input data.

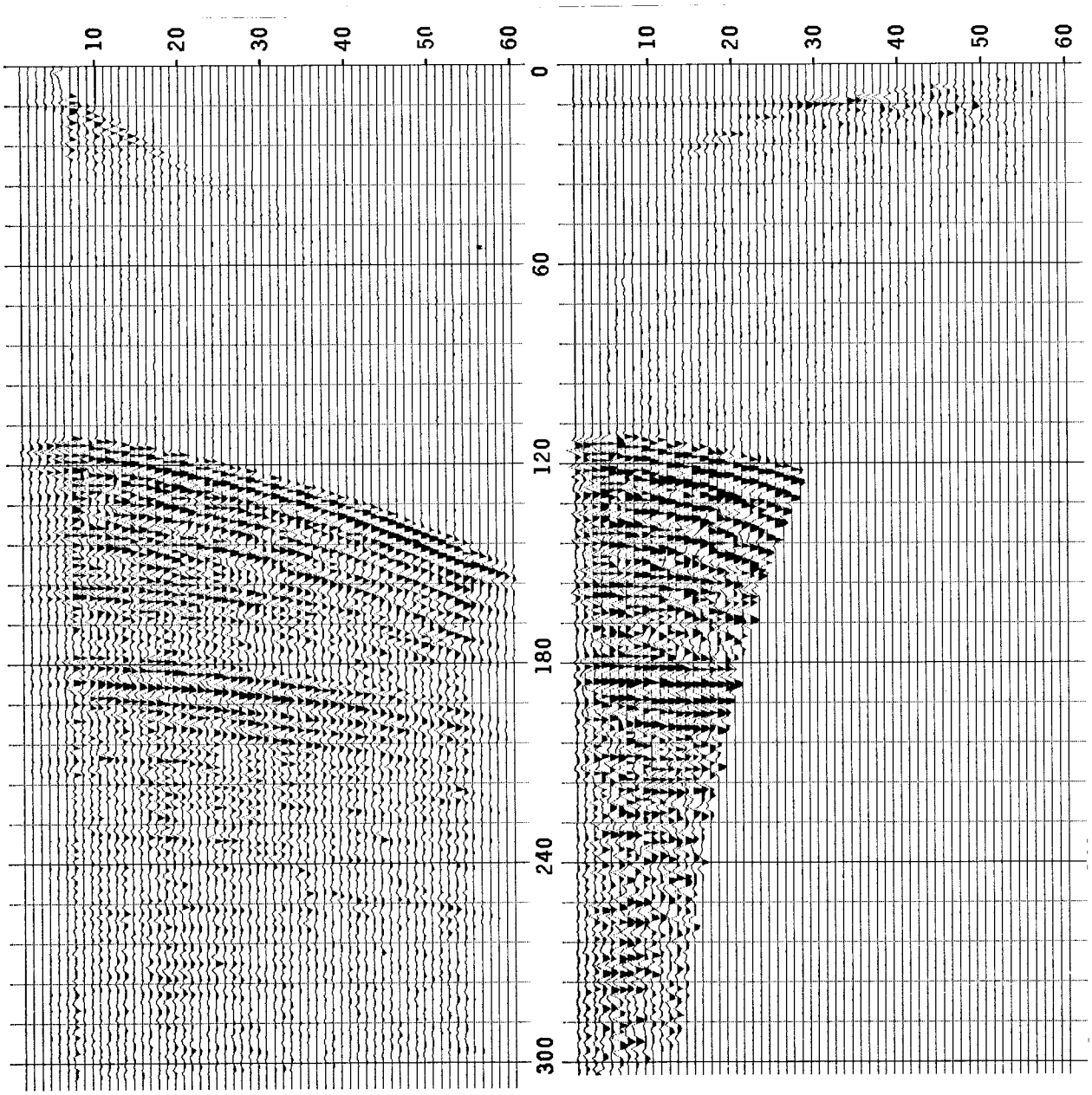

FIG. 10-11. Left: The data has been padded and extrapolated to suppress the truncation effects at far and near offsets. Right: The gather mapped into radial/NMO coordinates.

After extrapolation, the gather was gained to make it look as if it were recorded in a two dimensional world, and mapped into the radial/NMO coordinate system. The transformation velocity used was the minimum interval velocity corresponding to the rms velocity function which was the input to the transformation routine. If a larger transformation velocity is used, then there is a chance that some event will map into regions for which rv_0 exceeds unity. Since waves with ray parameters this large do not propagate, the choice of v_0 as the smallest interval velocity is the cheapest transformation velocity which does not artificially create evanescent energy.

To construct a mapping into the radial/NMO coordinate system, not only does a transformation velocity need to be specified, but some discretization parameters need to be chosen as well. The r axis was discretized so that there were as many sample points between $r = 0$ and $r = 1/v_0$ inclusive as points in the padded input. Similarly, the d axis was discretized so that there were as many sample points between $d = 0$ and the maximum depth expected inclusive as time samples in the input, scaled by the quotient of the maximum frequency in the signal by the Nyquist frequency.

The data as a function of r and d is plotted in figure 11. The result consists of a series of roughly horizontal bands. In general, the derivative with respect to r within such a band will be relatively small. Thus, the effect of undersampling the geophone axis has been effectively minimized by the transformation into NMO coordinates. This was expected, because the dips present on the near offset section were all less than ten degrees. The shortness of the bands is a bit more troublesome. The data at high d has almost certainly been undersampled. The only correction for this is to sample the r-axis at a higher rate and bear the increased cost of migration. The higher r values seem not to be present in the data, so one option which would decrease costs is to insist that the wave contain no events between some preset value r_0 and 1. Unfortunately, it is hard to tell if another gather than the one displayed might not contain an event with a large ray parameter or if any of the gathers of the line might not, after migration, contain such an event.

Finally, the gather was migrated and imaged. Plots of the image plane in r,d,z-space and the image in g,z-space appear in figures 12 and 13. Since Δz was chosen to be equal to 10 times Δd, the image plane's gradient was equal to 10 and lay in the plane $r = 0$. Only the volume beneath the image plane is involved in the migration process, due to the causality of the derivatives used in migration. The computational cost associated with downward continuing geophones is proportional to the volume of the active set beneath the image plane. It follows that choices of Δz smaller than the one used, even though they would have generated a cleaner image, involve much higher cost. The price paid for speed is the clutter at the image of the sea floor. As little oil can be expected to be trapped at the sea floor and

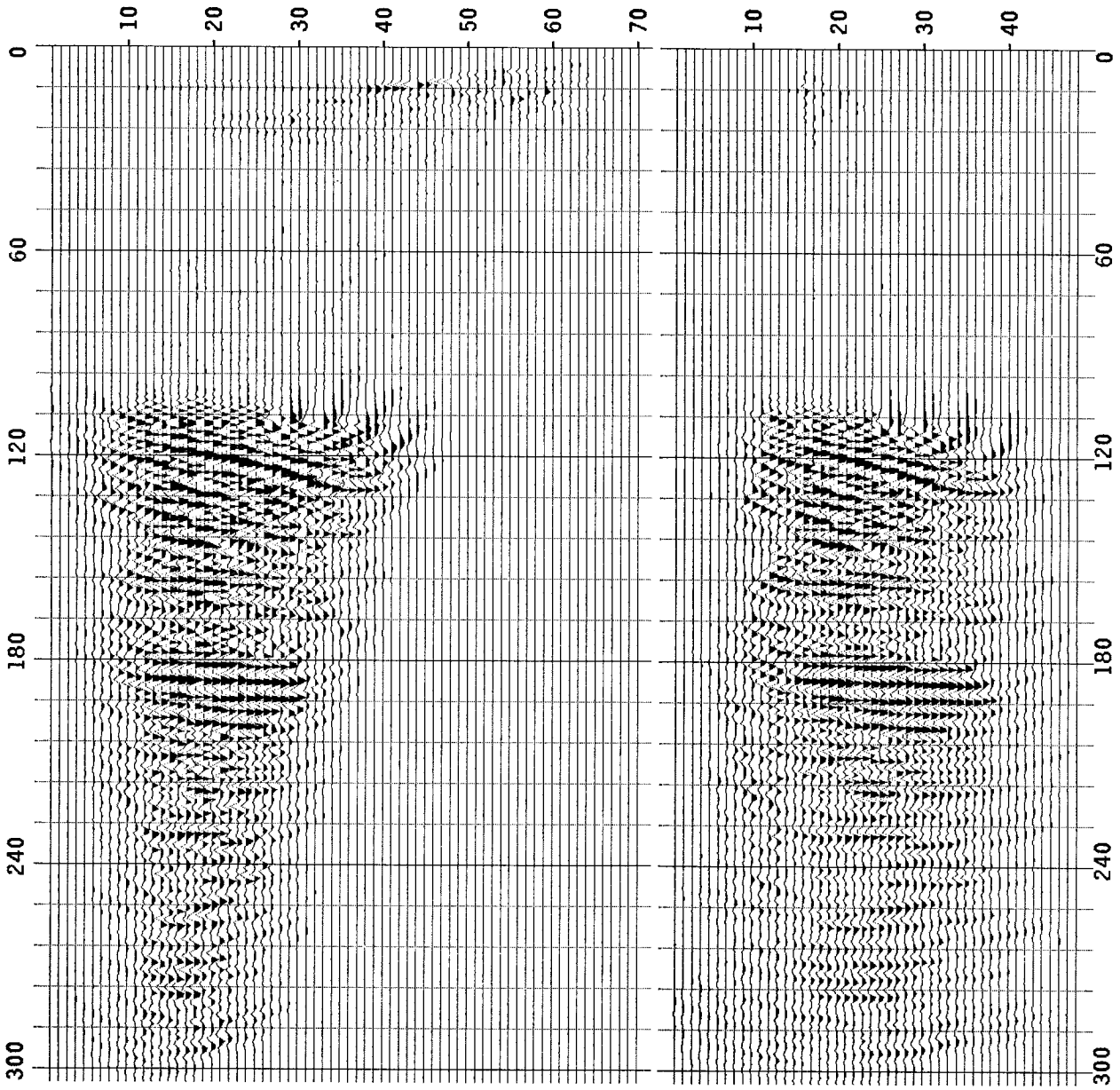

FIG. 12-13. Left: A migrated image plane in radial coordinates. Right: The image plane in the output coordinate system.

since the images of the other events seem clean, perhaps the large z step size is justified.

As promised, the common shot gathers of the USGS Gulf of Alaska line were migrated. Migrating a whole line of common shot gathers is much more interesting than migrating an isolated common shot gather because lateral velocity anomalies should be visible. If the data from the migrated common shot gathers are reorganized into common geophone gathers, then

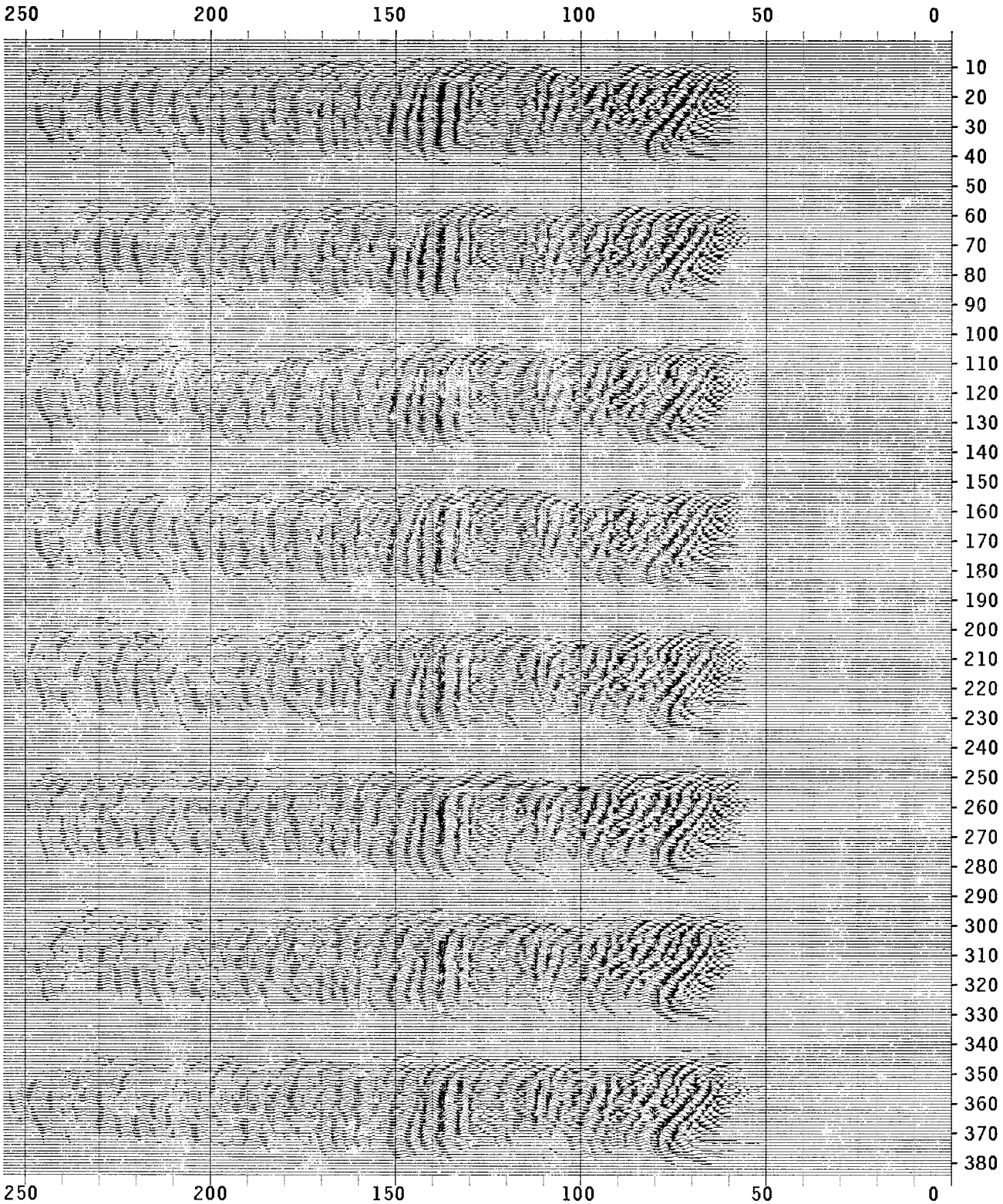

FIG. 14. The first eight gathers of the USGS Gulf of Alaska line. The gathers have been migrated in radial/NMO coordinates. The vertical axis has been sampled every 18.5 meters. The first sample plotted is the 49th, corresponding to a depth of 888 meters.

Plot	Nh	Dh	Nv	Dv	Interpretation
6	48	50 m	1250	4 ms	Input
7	48	50 m	1250	4 ms	NMO with rms v(t)
8	48	50 m	304	12.5 ms	Time to depth stretch
9	48	50 m	304	12.5 ms	Inverse NMO with v_0
10	60	50 m	308	12.5 ms	Pad sides and data extension
11	60	.011 ms/m	304	18.5 m	Radial/NMO transformation
12	70	.011 ms/m	304	18.5 m	Image plane in r,d,z-space
13	48	50 m	304	18.5 m	Migrated output

TABLE 2. The number of horizontal samples of the plots listed are in the column under Nh. The column under Dh lists sampling rates for the horizontal axes. Similarly, Nv and Dv are the number of samples and sample interval for the various vertical axes.

pictures of the subsurface obtained with different illumination angles are obtained. If the shot gather images are made with a correct velocity estimate, then the depth estimates of the various reflectors will be independent of illumination. On the other hand, if the shot gather images are made with a slightly incorrect velocity estimate, then the depth estimates will be slightly illumination dependent. For instance, if the velocity is a little too high, then the depth estimates will be larger for big offsets than for small offsets. If these travel time anomalies can be estimated reliably, then they can be converted into perturbations of the migration velocity field. Some progress has been made in calculating these perturbations. The results will be published in a subsequent paper, hopefully the author's long overdue thesis.

With this in mind, the seismic line was migrated with the velocity plotted in figure 3. The first eight gathers are again plotted, this time in figure 14. The results are disappointing, because the migrated output and the NMO corrected input (plotted in figure 4) are nearly identical in regions where the image can be trusted. The amount of lateral movement for the range of dips present in this data set is negligible. Thus, the differences between NMO and migration on this data set consist largely of migration artifacts. These artifacts, as in the example considered above, are most prominent in the padding at the sides of the gathers and in the region just above the image of the sea floor.

ACKNOWLEDGMENTS

Al Snyder revived the long dormant idea of common shot gather migration some three years ago. Discussions with Francis Muir started my own efforts towards migrating common shot gathers. Jon Claerbout invented the radial/NMO coordinate system for the migration of common shot gathers at the low cost and high speed demanded by industry. Conversations with Dave Hale have proven enlightening throughout.

****

26.

Four couples assembled together
To share an afternoon meal.
They gathered around a round table
Piled high with roast beef and veal.
Though every man sat 'twixt two women,
No man sat next to his mate.
From the following clues that I give you,
Can you figure where each of them sat?
Tyrone sat across from the pilot
And next to the demure Mrs. Tews.
George's wife worked each day as a jeweler
And he spent his time selling shoes.
Delane, he taught shorthand and typing.
The author was named Mary Jane.
Harry sat facing the doctor
And at left of sweet Mrs. Delane.
Mr. Tews had his dinner alongside
The photographer and Betty Kay.
Loretta's name was Van Allen;
The only blonde was Renee.
Ed sat at right of a Collins.
A lawyer was one of the bunch.
From only the clues I have given,
Can you figure where each one ate lunch?

****

27. Two days ago, I was only twenty-eight, but next year I'll be thirty-one. When's my birthday?

****

28. What eight-letter word contains five consecutive vowels? The first letter is q.